Bioorganic & Medicinal Chemistry Letters xxx (2016) xxx–xxx

Contents lists available at ScienceDirect

Bioorganic & Medicinal Chemistry Letters

journal homepage: www.elsevier.com/locate/bmcl

Design and synthesis of fused bicyclic inhibitors targeting the L5 loop site of centromere-associated protein E

Takaharu Hirayama *, Masanori Okaniwa *, Hiroshi Banno, Hiroyuki Kakei, Akihiro Ohashi, Momoko Ohori, Tadahiro Nambu, Kenichi Iwai, Tomohiro Kawamoto, Akihiro Yokota, Maki Miyamoto, Tomoyasu Ishikawa

Pharmaceutical Research Division, Takeda Pharmaceutical Company Limited, 26-1, Muraoka-Higashi 2-chome, Fujisawa, Kanagawa 251-8555, Japan

ARTICLE INFO

Article history:
Received 26 May 2016
Accepted 19 July 2016
Available online xxxx

Keywords:
CENP-E
Electrostatic potential map (EPM)
2,3-Dihydro-1-benzothiophene 1,1-dioxide derivatives
Anti-cancer agent
Anti-mitotic agent

ABSTRACT

Centromere-associated protein-E (CENP-E) is a mitotic kinesin which plays roles in cell division, and is regarded as a promising therapeutic target for the next generation of anti-mitotic agents. We designed novel fused bicyclic CENP-E inhibitors starting from previous reported dihydrobenzofuran derivative **(*S*)-(+)-1**. Our design concept was to adjust the electron density distribution on the benzene ring of the dihydrobenzofuran moiety to increase the positive charge for targeting the negatively charged L5 loop of CENP-E, using predictions from electrostatic potential map (EPM) analysis. For the efficient synthesis of our 2,3-dihydro-1-benzothiophene 1,1-dioxide derivatives, a new synthetic method was developed. As a result, we discovered 6-cyano-7-trifluoromethyl-2,3-dihydro-1-benzothiophene 1,1-dioxide derivative **(+)-5d** (**Compound A**) as a potent CENP-E inhibitor with promising potential for in vivo activity. In this Letter, we discuss the design and synthetic strategy used in the discovery of **(+)-5d** and structure–activity relationships for its analogs possessing various fused bicyclic L5 binding moieties.

Centromere-associated protein-E (CENP-E) is a mitotic spindle motor protein of the kinesin superfamily[1–4] and is localized at the kinetochores of chromosomes.[1,5] CENP-E plays a crucial role in chromosome congression at the equator by capturing the microtubule.[6–11] Dysfunction of CENP-E causes the pole-proximal chromosomes by chromosomal misalignment, resulting in prolonged mitotic arrest and the consequent apoptosis. Based on these findings, CENP-E attracts as a drug discovery target for the next generation of cancer therapeutic drugs.[12–14] Recently, several small molecule CENP-E inhibitors have been reported to induce antiproliferative activities in cancer cells in preclinical studies, while the clinical potency of the CENP-E inhibitor is being evaluated in the early phase of the clinical trials.[15–20] In our previous work, we developed a novel slow-binding type of CENP-E inhibitor, **(+)-5d** (**Compound A**).[21] **Compound A** displays antiproliferative activity in various tumor cell lines as well as antitumor activity in a human cancer xenograft model in mice. In this study, we demonstrate the chemical profiles of **Compound A** and its derivatives. This information will be helpful to develop the chemical optimization of CENP-E inhibitors.

To date, we have reported the results of our drug discovery efforts on the imidazo[1,2-*a*]pyridine class of CENP-E inhibitors represented by **(*S*)-(+)-1** (CENP-E IC_{50}: 3.6 nM).[22] With the aim of further lead optimization starting from **(*S*)-(+)-1**, we applied EPM analysis to the fused bicyclic moiety binding to the L5 loop site of CENP-E. Here, we report the design and synthetic strategy employed in the discovery of compound **(+)-5d** as well as SAR for its analogs possessing various fused bicyclic L5 binding moieties.

A previously reported structure–activity relationships (SAR) study based on our hypothetical modeling pointed out the structurally significant molecular characteristics for potent CENP-E inhibition (Fig. 1): (1) introduction of a basic *N*,*N*-dimethylaminoethyl group achieves strong interaction with carboxylate of Glu186,[24] (2) a methoxy group inserted into the imidazo[1,2-*a*]pyridine ring provides high affinity for the core scaffold with Ile182 of CENP-E in a hydrophobic interaction manner by adjusting electron density distribution on the pyridine ring,[22] and (3) dihydrobenzofuran moiety of **1** is also quite important because bicyclic ring formation at the benzylic position produces a rigid molecular conformation and the two consequent enantiomers which are distinctively recognized by the ligand binding site, providing effective

Abbreviations: DIPEA, *N*,*N*-diisopropylethylamine; HATU, hexafluorophosphate *O*-(7-azabenzotriazol-1-yl)-*N*,*N*,*N*′,*N*′-tetramethyluronium; PD, pharmacodynamic.

* Corresponding authors. Tel.: +81 466 32 1160; fax: +81 466 29 4448 (T.H.); tel.: +81 466 32 1158 (M.O.).

E-mail addresses: takaharu.hirayama@takeda.com (T. Hirayama), masanori.okaniwa@takeda.com (M. Okaniwa).

http://dx.doi.org/10.1016/j.bmcl.2016.07.038
0960-894X/

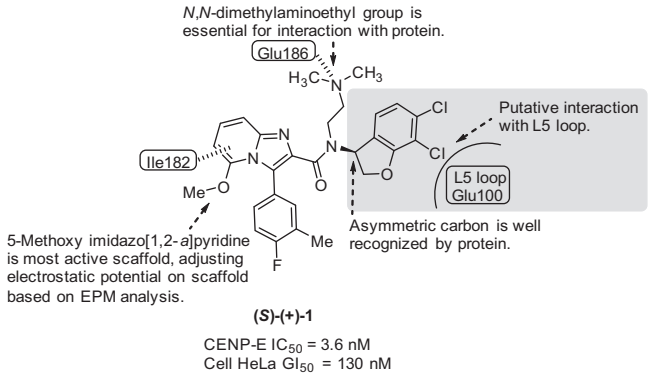

Figure 1. Chemical structure of lead compound **(*S*)-(+)-1** and SAR summary for imidazo[1,2-*a*]pyridine series.[22]

interaction of eutomer **(*S*)-(+)-1** with the L5 loop of CENP-E protein.

In this Letter, we thoroughly investigated chemical modification at the dihydrobenzofuran moiety. Our docking model of CENP-E indicated that the benzene ring of the dihydrobenzofuran moiety in **(*S*)-(+)-1** is located near the negatively charged carboxylate moiety of Glu100 in the L5 loop (shown in red, Fig. 2A). Therefore, our design concept for identifying an optimal CENP-E inhibitor was to

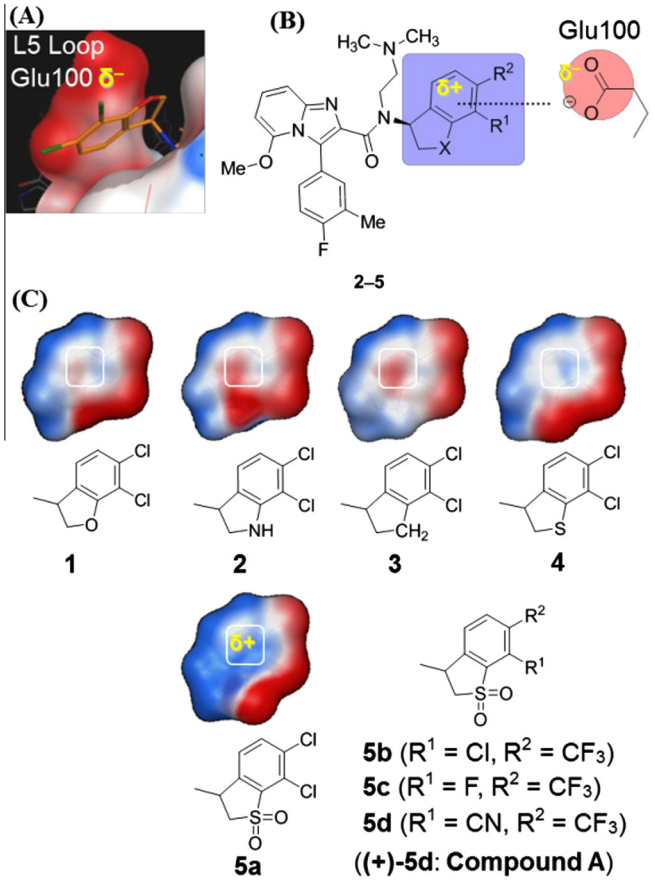

Figure 2. (A) Docking model of dihydrobenzofuran moiety of compound **(*S*)-(+)-1** with L5 Loop of CENP-E protein. (B) Plausible key interaction with negatively charged Glu100 of L5 Loop. (C) Design of compounds **2**–**5** and the EPM surfaces for the fused bicyclic scaffolds. The EPMs were calculated with MOE (version 2011.10).[23] Blue, red and white color indicate positive, negative and neutral charges, respectively. The benzene ring of the fused bicyclic scaffold is outlined by a white box.

adjust electron density distribution on the benzene ring to be positively charged by chemical modification of the fused bicyclic ring (Fig. 2B). Designed structures and their EPM views are described in Figure 2C: (1) selecting the optimal X atom of the fused bicyclic scaffold to induce positive charge on the benzene ring (compounds **2**–**5a**), (2) discovering the optimal combination of the electron withdrawing R^1 and R^2 groups on the benzene ring in a manner that maintains a favorable electrostatic profile (compounds **5b**–**d**) (Fig. 2C). According to EPM analysis of these newly designed compounds, 2,3-dihydro-1-benzothiophene derivative **4** (X = S), but not compounds **2** (X = NH) and **3** (X = CH_2), exhibited similar electrostatic potential to **1** (X = O). Furthermore, compound **5a** (X = SO_2) and its analogs (**5b**–**d**) clearly showed positively charged profiles, suggesting that this series of compounds could be anticipated to be optimal.

For the efficient synthesis of the promising series **(+)-5a**–**d**, robust synthetic methods were developed (Fig. 3). We applied two different approaches to prepare key intermediates **I**; (1) a conventional synthetic method via conjugate addition reaction[25] of benzothiophene 1,1-dioxide derivatives **II** with amines in Route A, and (2) newly developed synthetic method via one-pot imination and the following cyclization reaction of *o*-methanesulfonyl substituted benzaldehyde **V** in Route B.

The preparation methods for compounds **5a**–**d** are shown in Scheme 1. The condensation of 3-(4-fluoro-3-methylphenyl)-5-methoxyimidazo[1,2-*a*]pyridine-2-carboxylic acid **6**[22] with the key intermediate diamine derivatives **(±)-7a**–**d** using HATU in the presence of DIPEA or pyridine to give the corresponding racemic derivative **(±)-5a**–**d** in 68–80% yields. The optical resolution of racemic **(±)-5a**–**d** by a chiral HPLC gave two corresponding (+)- and (−)-enantiomers. Absolute configurations of the (+)-enantiomers were determined to be (*S*) by the single X-ray crystallographic analysis of representative compound **(+)-5d** (Fig. S1).

For the synthesis of amine derivatives (**I**) as the key intermediates, we initially adopted route A to prepare **(±)-7a**–**b**. The reduction of ketone derivatives **8a**,**b** with sodium borohydride provided alcohols **9a**,**b**. Alcohols **9a**,**b** were treated with boron trifluoride etherate ($BF_3{\cdot}Et_2O$) to give benzothiophene derivative **10a**, **b** in good yields. Subsequent oxidation of **10a**,**b** with hydrogen peroxide under the existence of a catalyst, sodium tungstate dihydrate, in AcOH and MeOH afforded benzothiophene 1,1-dioxide derivatives **11a**,**b** (precursor **II**) in high yields. The conjugate addition reaction of **11a**,**b** with *N*,*N*-dimethylethane-1,2-diamine provided desired diamine derivatives **(±)-7a**,**b** in 43% and 62% yields, respectively. Regarding **(±)-7c**,**d**, the preparation of **11c**,**d** (precursor **II**) was achieved in 4 steps from commercially available 1,2-difluoro-3-(trifluoromethyl)benzene **12c** and 2-fluoro-6-(trifluoromethyl)benzonitrile **12d**. Lithiation and subsequent formylation reaction assisted by neighboring group effect of fluorine atoms of **12c**,**d** successfully gave formylated derivatives **13c**,**d** in high yields. The reaction of **13c**,**d** with sodium methanesulfinate in DMSO provided methanesulfonyl derivatives **14c**,**d** in moderate yields. Next, the intramolecular cyclization reaction of **14c**,**d** by using sodium ethoxide in EtOH proceeded to give **15c**,**d**, followed by dehydration using MsCl under the existence of triethylamine in THF to give **11c**, **d** in good yields. Compound **(±)-7d** was synthesized in 43% yield in a synthetic method similar to that for **(±)-7a** (route A). On the other hand, conjugate addition of **11c** (R^1 = F, R^2 = CF_3) with *N*,*N*-dimethylethane-1,2-diamine unexpectedly did not provide the mixture of **(±)-7c**, but rather byproduct resulting from displacement of the fluorine group (R^1) of **11c** and additional byproduct containing *N*,*N*-dimethylethane-1,2-diamine introduced at the R^1 position of **(±)-7c**. This result motivated us to develop a one-pot imination-cyclization reaction (route B) to prepare **(±)-7c**. The one-pot imination of **14c** (precursor **V**) with *N*,*N*-dimethylethane-1,2-diamine in the presence of AcOH followed by intramolecular

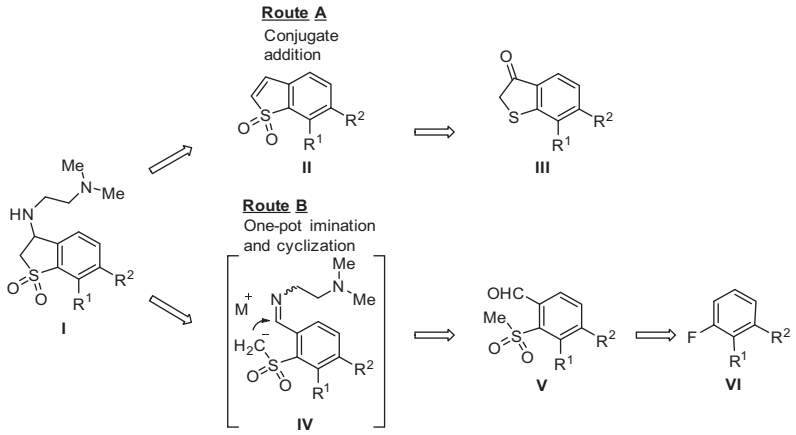

Figure 3. Retrosynthetic analysis of key intermediate diamine derivatives (I) via route A and our newly developed route B.

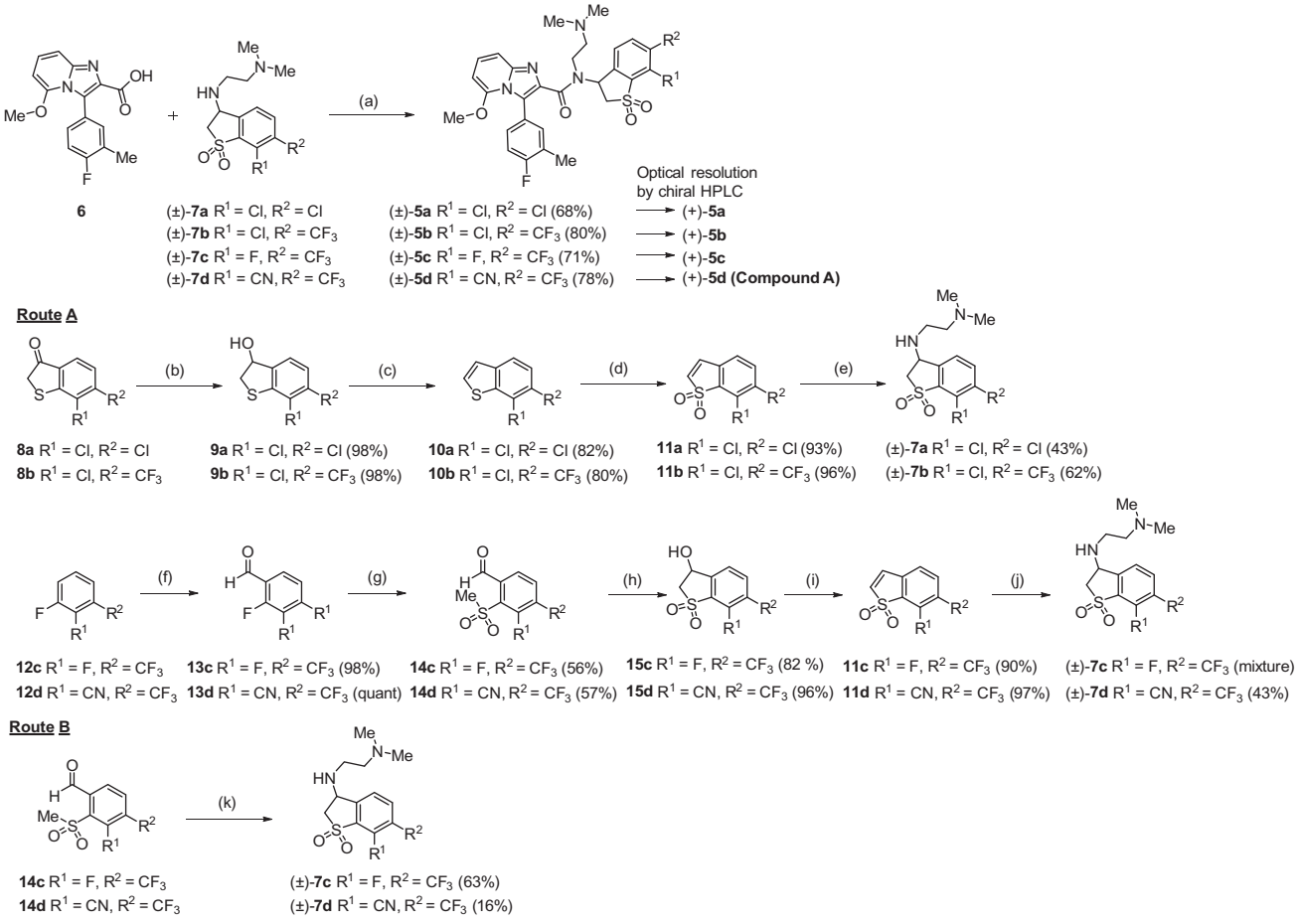

Scheme 1. Synthesis of **(+)-5a–d**, via route A or one-pot route B. Reagents and conditions: (a) HATU, pyridine, THF (for **(±)-5a**) or DIPEA, DMF (for **(±)-5b–d**), room temperature to 60 °C, 3 h–6 h. (b) Sodium borohydride, MeOH, 0 °C to room temperature, 1 h–4 h; (c) $BF_3{\cdot}Et_2O$, AcOH, room temperature, 0.25 h, then 100–120 °C, 0.3 h; (d) hydrogen peroxide, sodium tungstate dihydrate, AcOH, MeOH, 60–80 °C, 3 h–4 h; (e) *N*,*N*-dimethylethane-1,2-diamine, EtOH, 40 °C, 4 h then room temperature, 3 days (for **(±)-7a**) or ^{i}PrOH, 60 °C, 12 h (for **(±)-7b**). (f) 2,2,6,6-Tetramethylpiperidine, 1.6 M butyllithium in hexane, THF, −60 to −50 °C, 0.5 h, then *N*,*N*-dimethylformamide, −50 °C, 0.25 h, then to −10 °C, 0.5 h–1 h; (g) sodium methanesulfinate, DMSO, room temperature, 1.5 h–2 h; (h) NaOEt, EtOH, 0 °C to room temperature, 0.7 h–1 h; (i) MsCl, Et_3N, THF, 0 °C to room temperature, 0.5–4 h; (j) *N*,*N*-dimethylethane-1,2-diamine, EtOH, 70 °C, 4.5 h. (k) *N*,*N*-Dimethylethane-1,2-diamine, AcOH, THF, room temperature, 0.3 h–2 h, then 1.11 M LDA in hexane, 0 °C or −50 °C, 0.3 h–1 h.

cyclization using lithium diisopropylamide (LDA) was successfully conducted to yield the desired **(±)-7c** in 63% yield. Even when **14d** (R^1 = CN, R^2 = CF_3) was used as a starting material, this one-pot method proceeded to afford the desired **(±)-7d** in 16% yield. We expect that this facile one-pot synthetic method would be useful for constructing the 3-amino-2,3-dihydro-1-benzothiophene 1,1-dioxide scaffold as a pharmaceutical building block.

The results from evaluating the CENP-E ATPase inhibitory activity (IC_{50}) and cellular growth inhibitory activity (GI_{50}) in HeLa cells for compounds **1–5d** are summarized in Table 1. Compound **(±)-2**

Table 1
SAR for fused bicyclic compounds **1**–**4** and **5a**–**5d**

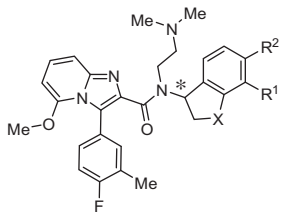

Compound	X	R^1	R^2	CENP-E IC_{50}[a] (nM)	HeLa GI_{50}[b] (nM)
(±)-1	O	Cl	Cl	4.8 (3.1–7.5)	270
(+)-1				3.6 (3.1–4.2)	130
(±)-2	NH	Cl	Cl	24 (16–37)	870
(±)-3	CH_2	Cl	Cl	19 (15–24)	>1000
(±)-4	S	Cl	Cl	14 (11–17)	850
(±)-5a	SO_2	Cl	Cl	2.7 (2.0–3.8)	160
(+)-5a				1.6 (1.2–2.1)	81
(+)-5b	SO_2	Cl	CF_3	1.7 (1.3–2.1)	110
(+)-5c	SO_2	F	CF_3	1.5 (1.3–1.8)	130
(+)-5d (**Compound A**)	SO_2	CN	CF_3	2.2 (1.9–2.6)	80

[a] $n = 2$. 95% confidence interval (CI) value.
[b] Cell proliferation of HeLa cells was determined by measuring cellular ATP amount ($n = 1$). Cells were collected 3 days after drug treatment.

(X = NH, IC_{50} = 24 nM) and **(±)-3** (X = CH_2, 19 nM) showed decreased CENP-E inhibitory activities compared to **(±)-1** (X = O, 4.8 nM). On the other hand, oxidized derivative **(±)-5a** (X = SO_2) showed potent CENP-E inhibition (IC_{50} = 2.7 nM) in contrast to unoxidized derivative **(±)-4** (X = S, IC_{50} = 14 nM). Consequently, the eutomer **(+)-5a** (IC_{50} = 1.6 nM, GI_{50} = 81 nM) was chosen as a lead compound for next SAR studies in which compounds with combinations of electron withdrawing R^1 and R^2 groups on the benzene ring were evaluated. Compounds **(+)-5b**–**5d** showed potent CENP-E inhibition (IC_{50} = 1.7 nM, 1.5 nM and 2.2 nM, respectively) comparable with **(+)-5a**. Among these compounds, **(+)-5a** (R^1, R^2 = Cl) and **(+)-5d** (R^1 = CN, R^2 = CF_3) demonstrated potent anti-proliferative activity against HeLa cells (GI_{50} = 81 nM and 80 nM, respectively).

We also performed cell cycle analysis by FACS to demonstrate if prolonged mitotic arrest was induced in response to **(+)-5a** and **(+)-5d** treatment, both of which exhibited a potent antiproliferative activity in HeLa cells. The FACS analysis revealed that treatments with these compounds was indeed induced phosphorylated histone H3 (p-HH3), a mitotic index, in a dose-dependent manner, and p-HH3 EC_{50} values of **(+)-5a** and **(+)-5d** were 79 and 39 nM, respectively (Table 2). Given that p-HH3 EC_{50} values are close to GI_{50} values in each compound, prolonged mitotic arrest could be responsible for antiproliferation in the cells treated with these compounds. Because **(+)-5a** and **(+)-5d** showed sufficient in vitro cellular potency, we selected these compounds as promising candidates for further in vivo evaluation. We measured the drug concentrations of tested compounds in both plasma and tumor, as well as accumulation levels of p-HH3 as an in vivo PD marker in a tumor xenograft model. After intraperitoneal (ip) administration with 100 mg/kg once a day (qd) in a human colorectal cancer Colo205 xenograft mouse model, **(+)-5d** showed higher levels of p-HH3 accumulation compared with **(+)-5a**. Drug concentration measurements found that compound **(+)-5d** showed better drug exposure in tumor than **(+)-5a** (Table 2). Based on these results, compound **(+)-5d** was selected as our CENP-E inhibitor candidate for further development.

In this Letter, we have described the rational design of fused bicyclic moiety targeting the L5 loop moiety of CENP-E using EPM analysis. A newly developed one-pot method for the preparation of 3-amino-2,3-dihydro-1-benzothiophene 1,1-dioxide scaffold proved to be facile and robust. Because compound **(*S*)-(+)-5d** demonstrated promising in vivo activity in single ip administration in a human Colo205 xenograft model in mice, we selected compound **(+)-5d** as our candidate possessing promising in vivo potential. As we have reported elsewhere, compound **(+)-5d** was used as an in vivo chemical tool designated as '**Compound A**' to investigate the unique molecular biology of cell death induced by CENP inhibition, which exhibits a different mechanism of action from that of another reported mitotic kinesin inhibitor, ispinesib.[20] Compound **(+)-5d** analogs are characterized by an ATP-competitive like mode of action, but with time-dependent inhibition profiles in which 1 h pre-incubation of compounds and CENP-E protein prior to ATP addition enhances inhibitory activities even at high ATP concentration in enzymatic assay.[22] This feature is different from the previously reported CENP-E inhibitor GSK923295A. Further characterization and in vivo pharmacology studies of **(+)-5d** were recently published.[21]

Acknowledgments

We thank to Hitoshi Kandori and Kentaro Iwata for toxicology and physicochemical evaluation; Yusuke Nakayama and Daisuke Morishita for the biological characterization of test compounds; Natsumi Fujii, Masako Nishimura, and Taeko Hattori for their assistance in chiral separation; and Mitsuyoshi Nishitani, Motoo Iida, and Yasumi Kumagai for their assistance in structure determinations (X-ray single crystal study along with deposition of data to the Cambridge Crystallographic Data Centre, and NMR study).

Supplementary data

Supplementary data (chemical synthesis procedures, biological enzymatic and cellular assay methods, in vivo assay method, calculation method for electrostatic potential map (EPM) analysis, and single-crystal X-ray structure analysis of **(+)-5d** (Fig. S1)) associated with this article can be found, in the online version, at http://dx.doi.org/10.1016/j.bmcl.2016.07.038.

Table 2
In vitro p-HH3 levels in HeLa cells, and pharmacokinetic profiles and p-HH3 levels in tumors in a Colo205 xenograft mouse model after treatment with **(+)-5a** and **(+)-5d**

Compound	In vitro p-HH3 EC_{50}[a] (nM)	Dose[b] (mg/kg)	Drug concentration		Accumulation of p-HH3 levels in tumor[d,e]
			Plasma[c,d] (μg/mL)	Tumor[c,d] (μg/g)	
(+)-5a	79	100	0.003	0.623	6.9
(+)-5d (**Compound A**)	39	100	0.047	9.121	22.2

[a] % of p-HH3 positive cells were determined using FACS in HeLa cells ($n = 3$).
[b] Dose of **(+)-5a** and **(+)-5d** is described. Compounds were treated by ip administration.
[c] Compound concentration in a Colo205 xenograft model in mice, 24 hours after the administration of **(+)-5a** and **(+)-5d**.
[d] Mean ($n = 2$).
[e] Phosphorylated HH3 in tumors was detected by Western blotting, 24 h after administration of **(+)-5a** and **(+)-5d**. Accumulation of p-HH3 levels were evaluated as band intensities based on vehicle.

References and notes

1. Miki, H.; Okada, Y.; Hirokawa, N. *Trends Cell Biol.* **2005**, *15*, 467.
2. Good, J. A. D.; Skoufias, D. A.; Kozielski, F. *Semin. Cell Dev. Biol.* **2011**, *22*, 935.
3. Huszar, D.; Theoclitou, M.-E.; Skolnik, J.; Herbst, R. *Cancer Metastasis Rev.* **2009**, *28*, 197.
4. Rath, O.; Kozielski, F. *Nat. Rev. Cancer* **2012**, *12*, 527.
5. Yen, T. J.; Li, G.; Schaar, B. T.; Szilak, I.; Cleveland, D. W. *Nature* **1992**, *359*, 536.
6. Wood, K. W.; Sakowicz, R.; Goldstein, L. S. B.; Cleveland, D. W. *Cell* **1997**, *91*, 357.
7. Schaar, B. T.; Chan, G. K. T.; Maddox, P.; Salmon, E. D.; Yen, T. J. *J. Cell Biol.* **1997**, *139*, 1373.
8. Sardar, H. S.; Luczak, V. G.; Lopez, M. M.; Lister, B. C.; Gilbert, S. P. *Curr. Biol.* **2010**, *20*, 1648.
9. Yao, X.; Anderson, K. L.; Cleveland, D. W. *J. Cell Biol.* **1997**, *139*, 435.
10. Barisic, M.; Aguiar, P.; Geley, S.; Maiato, H. *Nat. Cell Biol.* **2014**, *16*, 1249.
11. Barisic, M.; Silva e Sousa, R.; Tripathy, S. K.; Magiera, M. M.; Zaytsev, A. V.; Pereira, A. L.; Janke, C.; Grishchuk, E. L.; Maiato, H. *Science* **2015**, *348*, 799.
12. Jackson, J. R.; Patrick, D. R.; Dar, M. M.; Huang, P. S. *Nat. Rev. Cancer* **2007**, *7*, 107.
13. Chan, G. K.; Liu, S.-T.; Yen, T. J. *Trends Cell. Biol.* **2005**, *15*, 589.
14. Wood, K. W.; Chua, P.; Sutton, D.; Jackson, J. R. *Clin. Cancer Res.* **2008**, *14*, 7588.
15. Wood, K. W.; Lad, L.; Luo, L.; Qian, X.; Knight, S. D.; Nevins, N.; Brejc, K.; Sutton, D.; Gilmartin, A. G.; Chua, P. R.; Desai, R.; Schauer, S. P.; McNulty, D. E.; Annan, R. S.; Belmont, L. D.; Garcia, C.; Lee, Y.; Diamond, M. A.; Faucette, L. F.; Giardiniere, M.; Zhang, S.; Sun, C.-M.; Vidal, J. D.; Lichtsteiner, S.; Cornwell, W. D.; Greshock, J. D.; Wooster, R. F.; Finer, J. T.; Copeland, R. A.; Huang, P. S.; Morgans, D. J., Jr.; Dhanak, D.; Bergnes, G.; Sakowicz, R.; Jackson, J. R. *Proc. Natl. Acad. Sci. U.S.A.* **2010**, *107*, 5839.
16. Qian, X.; McDonald, A.; Zhou, H.-J.; Adams, N. D.; Parrish, C. A.; Duffy, K. J.; Fitch, D. M.; Tedesco, R.; Ashcraft, L. W.; Yao, B.; Jiang, H.; Huang, J. K.; Marin, M. V.; Aroyan, C. E.; Wang, J.; Ahmed, S.; Burgess, J. L.; Chaudhari, A. M.; Donatelli, C. A.; Darcy, M. G.; Ridgers, L. H.; Newlander, K. A.; Schmidt, S. J.; Chai, D.; Colón, M.; Zimmerman, M. N.; Lad, L.; Sakowicz, R.; Schauer, S.; Belmont, L.; Baliga, R.; Pierce, D. W.; Finer, J. T.; Wang, Z.; Morgan, B. P.; Morgans, D. J., Jr.; Auger, K. R.; Sung, C.-M.; Carson, J. D.; Luo, L.; Hugger, E. D.; Copeland, R. A.; Sutton, D.; Elliott, J. D.; Jackson, J. R.; Wood, K. W.; Dhanak, D.; Bergnes, G.; Knight, S. D. *ACS Med. Chem. Lett.* **2010**, *1*, 30.
17. Chung, V.; Heath, E. I.; Schelman, W. R.; Johnson, B. M.; Kirby, L. C.; Lynch, K. M.; Botbyl, J. D.; Lampkin, T. A.; Holen, K. D. *Cancer Chemother. Pharmacol.* **2012**, *69*, 733.
18. Bennett, A.; Bechi, B.; Tighe, A.; Thompson, S.; Procter, D. J.; Taylor, S. S. *Oncotarget* **2015**, *6*, 20921.
19. Kung, P. P.; Martinez, R.; Zhu, Z.; Zager, M.; Blasina, A.; Rymer, I.; Hallin, J.; Xu, M.; Carroll, C.; Chionis, J.; Wells, P.; Kozminski, K.; Fan, J.; Guicherit, O.; Huang, B.; Cui, M.; Liu, C.; Huang, Z.; Sistla, A.; Yang, J.; Murray, B. W. *Mol. Cancer Ther.* **2004**, *13*, 2104.
20. Ohashi, A.; Ohori, M.; Iwai, K.; Nakayama, Y.; Nambu, T.; Morishita, D.; Kawamoto, T.; Miyamoto, M.; Hirayama, T.; Okaniwa, M.; Banno, H.; Ishikawa, T.; Kandori, H.; Iwata, K. *Nat. Commun.* **2015**, *6*, 7668.
21. Ohashi, A.; Ohori, M.; Iwai, K.; Nambu, T.; Miyamoto, M.; Kawamoto, T.; Okaniwa, M. *PLoS ONE* **2015**, *10*, e0144675. http://dx.doi.org/10.1371/journal.pone.0144675.
22. Hirayama, T.; Okaniwa, M.; Banno, H.; Kakei, H.; Ohashi, A.; Iwai, K.; Ohori, M.; Mori, K.; Gotou, M.; Kawamoto, T.; Yokota, A.; Ishikawa, T. *J. Med. Chem.* **2015**, *58*, 8036.
23. *Molecular Operating Environment (MOE), 2011.10*; Chemical Computing Group: 1010 Sherbrooke St. West, Suite #910, Montreal, QC, Canada, H3A 2R7, 2011. www.chemcomp.com.
24. Hirayama, T.; Okaniwa, M.; Imada, T.; Ohashi, A.; Ohori, M.; Iwai, K.; Mori, K.; Kawamoto, T.; Yokota, A.; Tanaka, T.; Ishikawa, T. *Bioorg. Med. Chem.* **2013**, *21*, 5488.
25. Sauter, F.; Jordis, U.; Stanetty, P.; Hüttner, G.; Otruba, L. *Arch. Pharm.* **1981**, *314*, 567.